scientific reports

Check for updates

OPEN

# Effect of the pressureless post-sintering on the hot isostatic pressed $Al_2O_3$ prepared from the oxidized AlN powder

K. Balázsi[1]✉, D. Varanasi[1], Zs. E. Horváth[1], M. Furkó[1], F. S. Cinar[2] & C. Balázsi[1]

**The effect of the pressureless post-sintering in hydrogen on the structural and mechanical properties of the hot isostatic pressed $Al_2O_3$ prepared by oxidized AlN powder has been studied. The micrometer size AlN powder has been oxidized in air at 900° C and sintered by hot isostatic pressing (HIP) at 1700 °C, 20 MPa nitrogen atmosphere for 5 h. Pressureless sintering (PS) has been applied for all HIP sintered samples in $H_2$ gas at 1800° C for 10 h. It has been shown that the oxidation caused a core–shell AlN/$Al_2O_3$ structure and the amount of $Al_2O_3$ increased with increasing of the oxidation time of the AlN powder. For the first time, the green samples obtained from oxidized AlN powder have been successfully sintered first by HIP followed by post-sintering by PS under hydrogen without adding any sintering additives. All post-sintered samples exhibited the main α-$Al_2O_3$ phase. Sintering in $H_2$ caused the full transformation of AlN to α-$Al_2O_3$ phase and their better densification. Therefore, the hardness values of post-sintered samples have been increased to 17–18 GPa having apparent densities between 3.11 and 3.39 g/cm$^3$.**

Aluminum nitride (AlN) is an alternative refractory ceramic material being used in various range of applications such as optics, electronics and computer circuits for its unique thermal and electrical properties. It has a really high degree of thermal stability and wear resistance while exhibiting a low density[1]. AlN can be obtained either by carbo-thermal reduction of alumina ($Al_2O_3$) or by nitridization of aluminum (Al)[1,2]. AlN exhibits covalent bonding and generally has been sintered around temperatures higher than 1600 °C under the presence of sintering additives acting as oxygen absorbers[2]. On the other hand, $Al_2O_3$ is a simple covalent oxide of aluminum which is generally formed at the surface of pure aluminum. The growing trend of the key issue of the microstructure of the oxide layer and its effect on the oxidation behavior of AlN ceramics is still unclear[3,4]. $Al_2O_3$ has some known phase allotropes. The most commonly identified phase although other intermediary phases evolve during the oxidation process is the γ-$Al_2O_3$[5]. However, these phases are mostly unstable and disintegrate at higher temperatures[5]. These thin aluminum oxide films have been increasingly used in various types of electronic devices as dielectric and tunneling barriers[6]. Zheng et al. fabricated the AlN-$Al_2O_3$ composite ceramic by heat treating $Al_4O_4C$ porous ceramic under $N_2$ atmosphere above 1500 °C. They showed, that the granular AlN and $Al_2O_3$ particles integrated with each other and closely connected at their grain boundary[7]. Oxidation of AlN ceramics is complicated because of the process is influenced by various factors[8]. Moreover, the oxidation of AlN has been shown to lead to improvements in the adhesion of deposited metal layers in several electronic package applications[8]. Yeh et al. studied the oxidation mechanism of AlN particles through microstructure observation[9]. They confirmed the formation of porous oxide layer on the surface of AlN. The oxidation kinetics was therefore fast and this reaction induced an increased in thickness of oxide layer. The reaction stopped when the pores were no longer interconnected. Korbutowicz et al. studied the oxidation rates of aluminum nitride thin films[10]. They observed the quick diffusion and the oxygen gradient in AlN layers: aluminum nitride inside has been infected with oxygen, due to the surface of aluminum oxide layer revealed a high porosity. The mentioned results are in good agreement with investigations made by Zheng et al.[9]. Maghsoudipour et al. investigated the oxidation behavior of AlN samples in air at elevated temperatures up to 1300 °C gaining different amounts of $Al_2O_3$[11]. The amount of AlN and AlON phases in samples controlled the oxidation behavior of such composites. In samples, having high amount of AlN, the high volume of the evolved nitrogen gas can crack the sample causing further

[1]Thin Film Physics Department, Institute of Technical Physics and Materials Science, Centre for Energy Research, Konkoly-Thege M. Str. 29-33, Budapest 1121, Hungary. [2]Metallurgical and Materials Engineering Department, 34469 Maslak, Istanbul, Turkey. ✉email: balazsi.katalin@ek-cer.hu

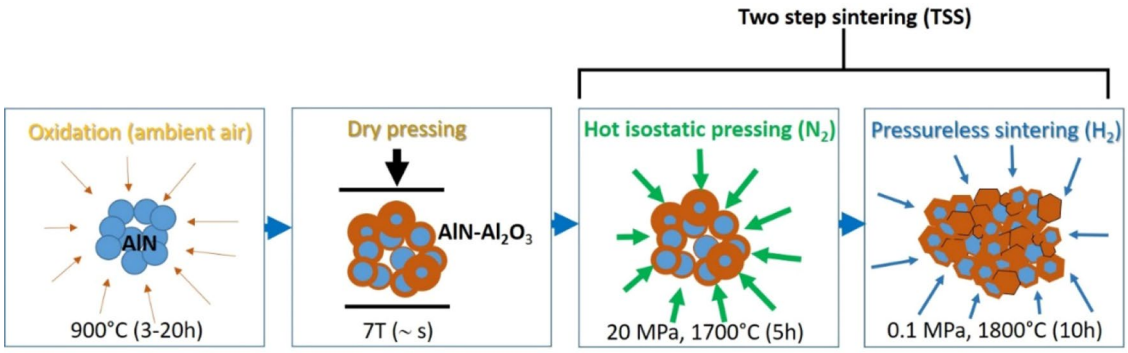


**Figure 1.** Experimental procedure of $Al_2O_3$ sintered sample preparation from AlN powder.

oxidation. Cao et al. also investigated the mechanism of $Al_2O_3$ core formation in AlN films during oxidations[12]. A core–shell structure composed of the AlN core wrapped in the continuous $Al_2O_3$ shell layer has been formed with weak bonding between the core/shell interface and neighboring $Al_2O_3$ shells. The sintering process is more difficult especially for AlN ceramic. The sintering temperature and time must be suitable for each composition (AlN or $Al_2O_3$). On the other hand, the processing method is influencing the obtained microstructure, reduces the grain size and increases the densification of final sintered ceramic. Hot isostatic pressing (HIP) has unique advantages in promoting the compactness of parts, eliminating void defects, reducing segregation and improving the mechanical properties of the ceramics. The presence of more vacancies and pores in oxide core layer can enhance the sintering by offering a higher chance for lattice diffusion[13]. The HIP sintering of $Al_2O_3$ ceramics has a long history of development, therefore is the most familiar for use in the processing of the many existing ceramics materials[14]. Prosvirnin et al. communicated that in the production of oxynitride ceramics micro-additives of sintering components such as $Y_2O_3$, $La_2O_3$, and others are used[15]. The main sintering additive used in oxynitride ceramics is $Y_2O_3$, which has excellent physical and chemical properties, such as high melting point (2430° C) and the density is 5.01 g $cm^{-3}$[15]. Its presence can facilitate the liquid phase during sintering, which is beneficial for compacting and removing pores. Varanasi et al. first oxidized AlN powders for 3, 10 or 20 h and after that sintered by HIP for the first time the dense AlN-$Al_2O_3$ composite without $Y_2O_3$ sintering additives[16]. The sintered samples showed the presence of only α-$Al_2O_3$ besides AlN proving that the sintering results in disintegration of θ-$Al_2O_3$ phase. Their experiments also provided that the densification of sintered ceramics can be achieved by HIP at lower temperatures[16].

Hydrogen can facilitate the detachment of protective oxide layer from the metals and alloys. The degradation is usually accelerated at elevated temperatures in many industrial applications[17]. Li et al. studied the effect of hydrogen on the integrity of aluminum–oxide interface at elevated temperatures[17]. Anya et al. used the pressureless sintering in hydrogen to obtain $Al_2O_3$-SiC composites[18]. They reported exploration of the effects of sintering variables on the final density and resultant Young's modulus of composites. Taun et al. prepared the $Al_2O_3$-Ni composites by pressureless sintering in $H_2$[19]. The sintering had certain effects on mechanical properties of the composites. The toughness of the composites is enhanced by a crack bridging mechanism or by microcrack toughening. However, the strength of the composites is decreased significantly as the microcracks are formed[19]. Our previous study of the structural and mechanical characterizations of HIP sintered AlN-$Al_2O_3$ was discussed in[16]. A combination of HIP and PS post-sintering is proposed in this paper to obtain high-density bodies with higher hardness. In this work, the effect of pressureless sintering in hydrogen on hot isostatic pressed AlN-$Al_2O_3$ prepared from oxidized AlN powder was studied.

## Materials and experimental

Base AlN ceramic powders with purity of 98 wt% and the average size of 1.3 ± 0.5 µm (H.C. Starck GMBH, Berlin) have been oxidized in ambient atmosphere at 900 °C for 3, 6, 10 and 20 h respectively. The oxidized AlN powders have been pressed by dry press at 7t. After it, the green bodies have been embedded to BN powder in a graphite crucible and sintered by hot isostatic pressing (HIP, ABRA type) at pressure of 20 MPa, at 1700 °C in an inert gas ($N_2$) environment for 5 h. As a post-sintering step, the HIP sintered ceramics have been pressureless sintered (PS) at 1800 °C for 10 h under $H_2$ environment simultaneously applying 0.1 MPa pressure. The schematic view of experimental procedure is shown in Fig. 1.

The morphology and the microstructure of the powders and sintered samples have been characterized by scanning electron microscopy (SEM). Leo 1540XH Gemini with lens under SEM-SE mode has been used for the powders and Thermo-scientific Scios 2 for the sintered samples. The surface of the sintered samples have been covered by thin carbon coating to have better resolution and conduction. X-ray diffractometry (XRD) has been carried out using Bruker AXS D8 Discover diffractometer for phase analysis of both the powders and sintered samples. The numbering of the samples after each preparation processes has been indicated in Table 1.

The apparent density of the sintered samples has been measured using Archimedes method where the samples with surface porosity have been immersed in soap water for three days ensuring the complete filling of the pores. The equation used for calculation has been provided in Eq. (1).

| Oxidation time (h) | Oxidized AlN | HIP sintered AlN-$Al_2O_3$ | Pressureless sintered ceramics |
|---|---|---|---|
| 0 | O_0 | HIP_0 | PS_0 |
| 3 | O_3 | HIP_3 | PS_3 |
| 6 | O_6 | HIP_6 | PS_6 |
| 10 | O_10 | HIP_10 | PS_10 |
| 20 | O_20 | HIP_20 | PS_20 |

**Table 1.** Identification of samples after each preparation processes.

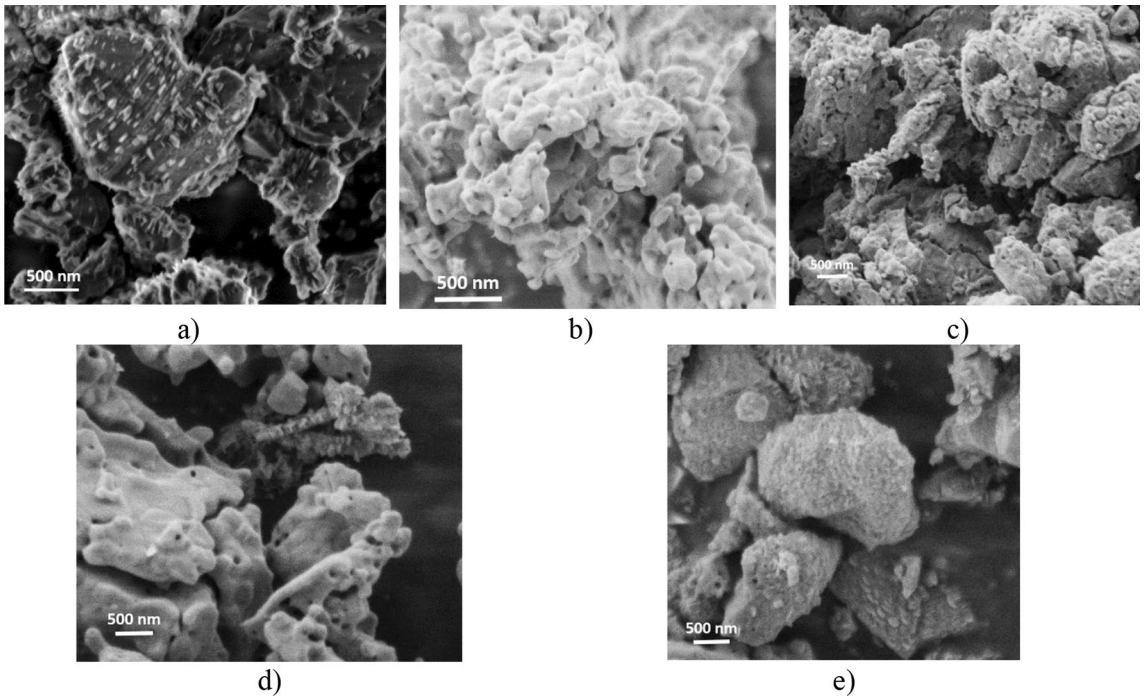


**Figure 2.** Morphological investigations of oxidized AlN powders. (**a**) reference—without oxidization (O_0), (**b**) 3 h oxidization (O_3), (**c**) 6 h oxidization (O_6), (**d**) 10 h oxidization (O_10) and (**e**) 20 h oxidization (O_20).

$$\rho_{\text{apparent}} = \frac{\text{wt of dry sample}}{\text{wt of dry sample} - \text{wt of immersed sample}} \cdot \rho_{\text{water}} \quad (1)$$

The hardness tests of the sintered (HIP and PS) samples have been carried out using Leitz Wetzlar 721464 Vickers microhardness equipment under a load of 19.61 N (2000 P) and the required calculations have been done according to the following equation, Eq. (2),

$$H_v = \frac{1.89 \cdot F \cdot 10^3}{d^2} \quad (2)$$

where $H_v$ is the Vickers hardness, F is the applied force (N) and d is the diagonal length (mm).

## Results and discussion

**Morphological investigations of the powders and the sintered samples.** The oxidation behavior of AlN is an important issue. The intermediate unstable phases as δ-$Al_2O_3$, θ-$Al_2O_3$ can be developed during the transformation of AlN to $Al_2O_3$[20]. The studies confirmed that the oxidation mechanism may be described as a reaction process together with a diffusion process. The oxidation process for AlN has been founded in temperatures ranging from 550 to 1100 °C[21–24]. The nearly globular micrometer sized AlN powder has been oxidized at 900 °C from 3 to 20 h in ambient atmosphere (Fig. 2). AlN powder before oxidation showed mainly globular character with average grain size of ~ 1 µm (Fig. 2a). The presence of only the AlN phase has been confirmed by the elemental composition (Fig. 3) analysis. No morphological changes after 3 h oxidization (Fig. 2b) have been observed. The EDS confirmed the presence of oxygen (Fig. 3a) and the quantitative analysis proved the AlN : $Al_2O_3$ ratio to be 19 : 81 wt% (Fig. 3b). Increasing of oxidation time to 6 h slightly increased the grain size of oxidized AlN (Fig. 2c) and the AlN : $Al_2O_3$ ratio is 4 : 96 wt% (Fig. 3).

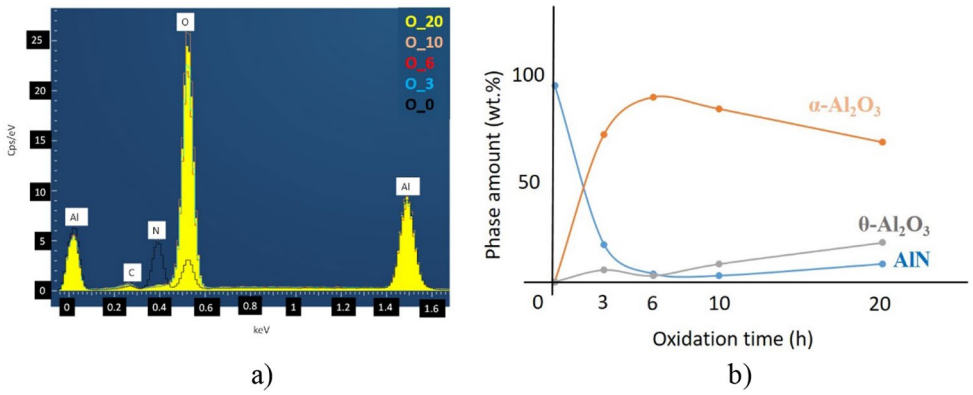


**Figure 3.** Elemental composition of oxidized AlN. (**a**) Elemental map of powders*, (**b**) quantitative results calculated from XRD. *C is a contamination from carbon tape.

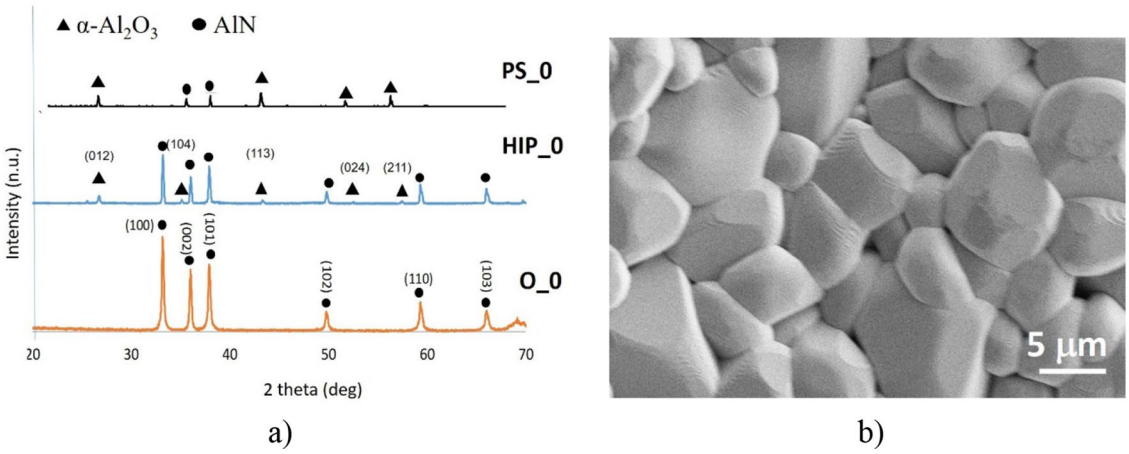


**Figure 4.** Investigation of AlN reference. (**a**) XRD plots of reference AlN powder (O_0), HIP sintered (HIP_0) and sintered at $H_2$ (PS_0), (**b**) SEM image of PS_0.

The increasing of the oxidization time above 10 h caused the formation of pores on the surface of the AlN, indicating the creation of $Al_2O_3$ oxide phase (Fig. 2d,e). The results are in good agreement with the works of Maghsoudipour et al.[11] and Cao et al.[12]. The particle clustering can also be observed in cases of samples with oxidization time above 6 h.

In our previous study, it has been confirmed simultaneous growth of two different phases of aluminum oxide, α-$Al_2O_3$ and the intermediary θ-$Al_2O_3$ (Fig. 3b). Although the second phase of aluminum oxide can be observed only in the powders after 10 and 20 h of oxidation time[16]. These measurements are in agreement with Tabary et al.[20].

Sintering of $Al_2O_3$ ceramics by hot isostatic pressing (HIP) has a long history[25]. The advantage of HIP over conventional sintering processes is in obtaining of the very high dense samples. In the case of HIP_10 and HIP_20, the presence of α-$Al_2O_3$ phase has been only observed. It can be explicable by the sintering process in nitrogen and high temperature disintegrated the non-stable θ-$Al_2O_3$ phase[16]. As a post-sintering step pressureless sintering (PS) in hydrogen was applied to as processed HIP samples. Pressureless sintering of AlN-$Al_2O_3$ has been applied to further densify the samples with complex shapes after HIP sintering. The sintered samples (PS_3–PS_20) have been heated at 1800 °C, 0.1 MPa under $H_2$ environment to complete the conversion cycle of AlN to $Al_2O_3$.

Comparison of the phase composition of the oxidized powders, HIP sintered and PS sintered samples have been performed by X-ray diffractometry (XRD) (Figs. 4a, 5a, 6a, 7a, 8a). In all samples, hexagonal AlN (JCP2:03–065-1902) and uniform rhombohedral α-$Al_2O_3$ (JCP2:00–010–0173) have been observed as major phases. The oxidation of AlN powders created two new distinct phases of aluminum oxide; major α-$Al_2O_3$ and minor θ-$Al_2O_3$, as it has been shown in our previous work[16]. During the oxidation of AlN, besides α-$Al_2O_3$, formation of various intermediary phases of aluminum oxide, like θ-$Al_2O_3$ and γ-$Al_2O_3$ were observed. However, these oxide phases are unstable and disintegrate at temperatures above 1100 °C[26,27].

The phase and structural transformation of pure AlN (Fig. 2a) without oxidation has been studied as reference (Fig. 4). The transformation of the part of the AlN to α-$Al_2O_3$ during HIP sintering (Fig. 4b) has been observed. The subsequent PS sintering effected the grain growth from 1 µm to ~ 5 µm (Fig. 4b) at 1800 °C for 10 h. Besson

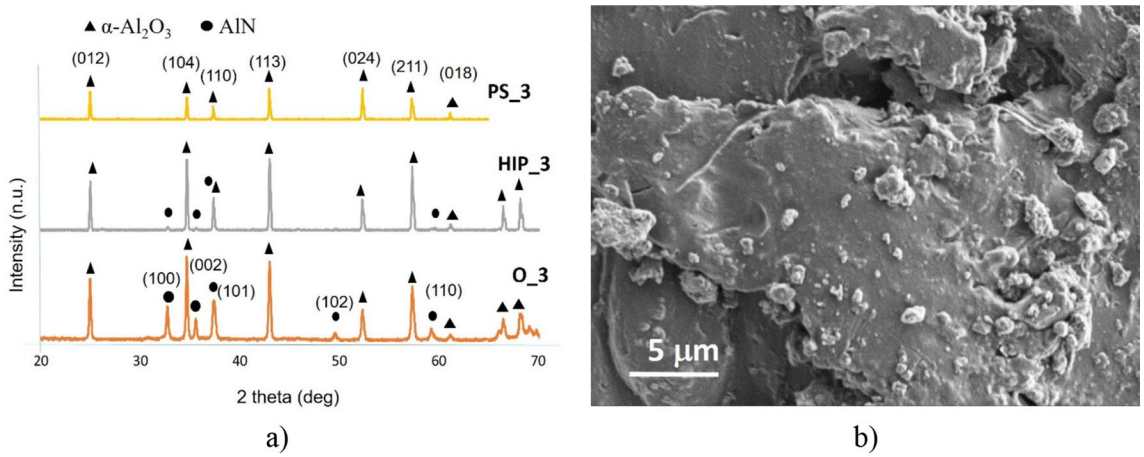


**Figure 5.** Investigation of oxidized AlN at 3 h. (**a**) XRD plots of oxidized AlN powder (O_3), HIP sintered (HIP_3) and sintered at $H_2$ (PS_3), (**b**) SEM image of PS_3.

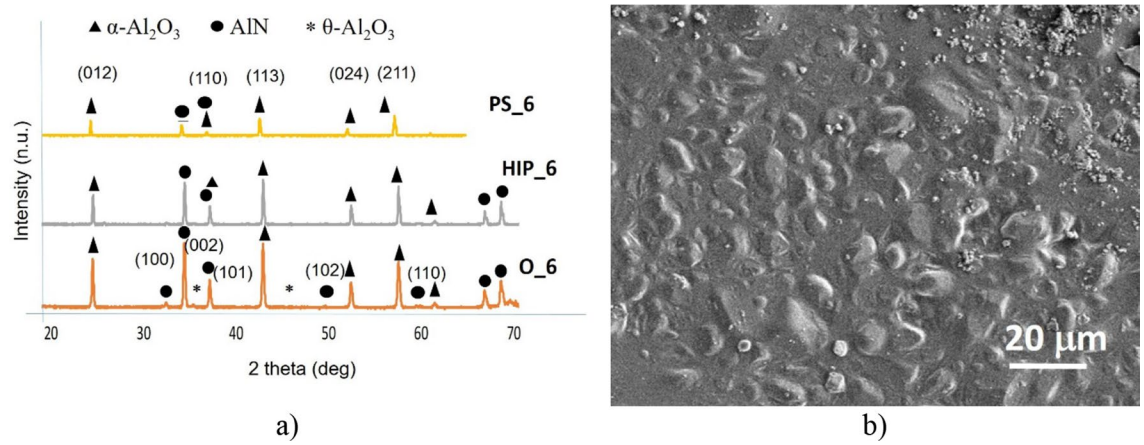


**Figure 6.** Investigation of oxidized AlN at 6 h. (**a**) XRD plots of oxidized AlN powder (O_6), HIP sintered (HIP_6) and sintered at $H_2$ (PS_6), (**b**) SEM image of PS_6.

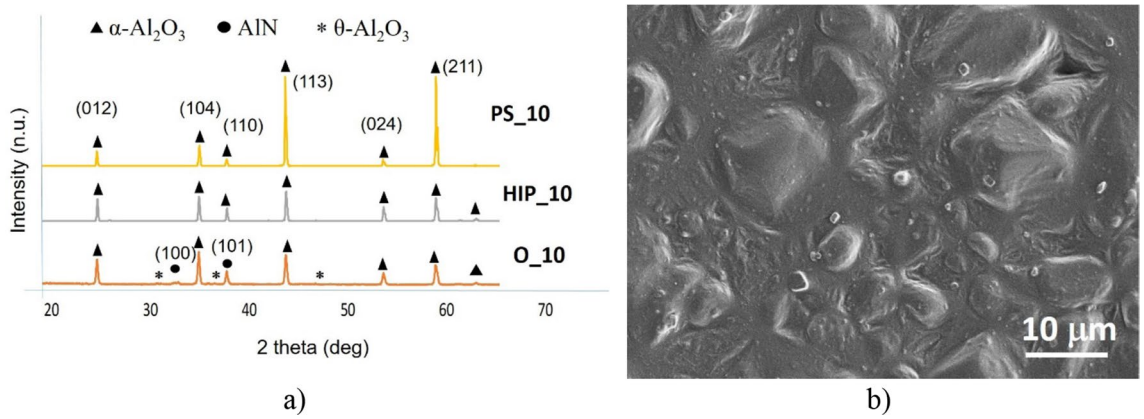


**Figure 7.** Investigation of oxidized AlN at 10 h. (**a**) XRD plots of oxidized AlN powder (O_10), HIP sintered (HIP_10) and sintered at $H_2$ (PS_10), (**b**) SEM image of PS_10.

and Abouaf reported that this effect has not been observed only if the pressureless sintering prolonged 100 h at the temperature of 1400 °C[28].

The comparative phase analysis of the 3 h oxidized AlN and HIP-post PS processes have been presented in Fig. 5. The higher volume of α-$Al_2O_3$ (Fig. 3b) helped the strong phase transformation of remnant AlN to α-$Al_2O_3$ and the sintering in $H_2$ finished this process (Fig. 5a). This fact has been confirmed by the XRD results (Fig. 5a).

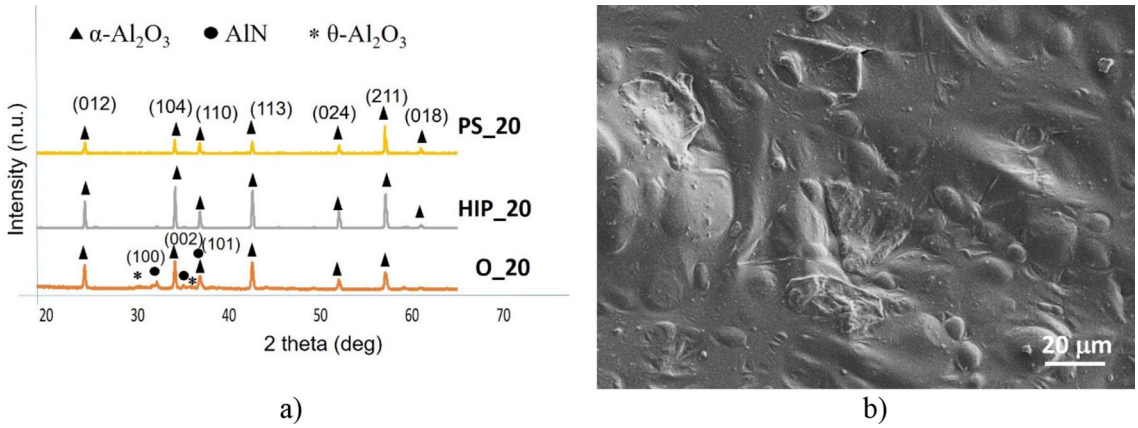


**Figure 8.** Investigation of oxidized AlN at 20 h. (**a**) XRD plots of oxidized AlN powder (O_20), HIP sintered (HIP_20) and sintered at $H_2$ (PS_20), (**b**) SEM image of PS_20.

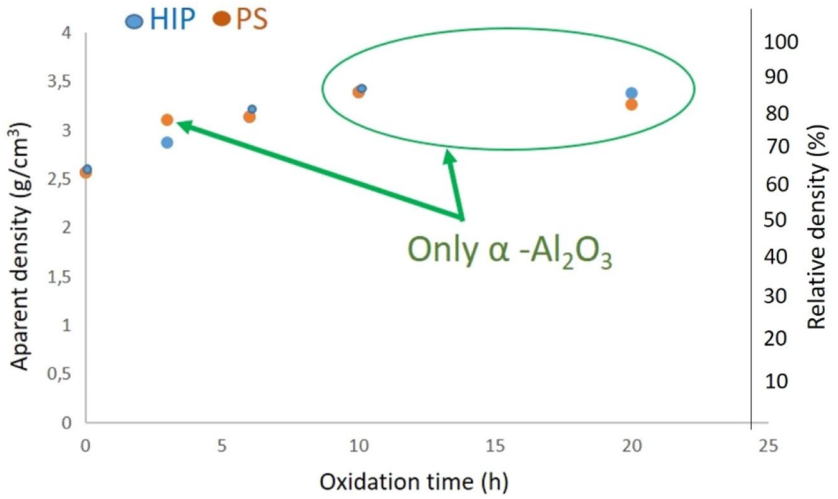


**Figure 9.** Apparent and relative density measurements of the HIP and PS samples.

The major reflections corresponding to stable α-$Al_2O_3$ phase occured at 25°, 35°, 43°, 52° and 57° 2θ positions. The PS sintered $Al_2O_3$ has been consisted from the non-uniform morphology (Fig. 5b). The grain size has been still around 5 µm but compared to non-oxidized reference (Fig. 4b), the surface was smoother.

Oxidation above 6 h induced the presence of intermediary θ-$Al_2O_3$ phase. This phase could be topotactically transformed from γ-$Al_2O_3$, which is stable under higher heat-treatment temperatures 800 °C[29]. θ-$Al_2O_3$ is more stable at higher temperatures of ~ 950–1000 °C where kinetic factors play a lesser role[29]. The HIP and PS as well are using comparable higher sintering temperatures, which occured the transformation of the metastable θ-$Al_2O_3$ (Fig. 6a). XRD measurements confirmed mainly α-$Al_2O_3$ with minor AlN phase (Fig. 6a). The morphology of PS sintered sample is shown in Fig. 6b, the sample is characterized by the average grain size ~ 5 µm.

The oxidization above 10 h had the effect on content of AlN. This fact has been supported by the phase and morphological study illustrated in Figs. 7 and 8. In both cases, the presence of metastable θ-$Al_2O_3$ have been proved after oxidation (Figs. 7a, 8a). In all the sintered samples, the composition of $Al_2O_3$ increased as function of oxidation time. The second heating cycle (PS) eliminated all intermediary oxide phases and transformed the substrate into a uniform α-$Al_2O_3$ phase. Therefore, combined sintering (HIP + PS) associated with complete conversion of base AlN to $Al_2O_3$ (Corundum) in the case of longer oxidation time. „The grain size of post-sintered ceramics slightly increased to 10–20 µm in the case of 10 h or 20 h oxidation times."

The apparent density measurement can help in the valuable information to control the quality of a ceramic with respect to the porosity. The apparent densities of sintered samples (HIP, PS) are shown in Fig. 9. The comparative study of densities of HIP sintered and PS sintered samples showed the similar tendency. The HIP and PS sintered base (reference) AlN exhibited the lowest apparent density (2.57 g/cm$^3$, Fig. 9). Increasing of the oxidation time of base AlN powder caused the increasing of density values from 2.87 to 3.38 g/cm$^3$ for HIP_3-20 and from 3.11 to 3.27 g/cm$^3$ for PS_3-20, respectively. Kim et al. developed the $Al_2O_3$ with additions of 1–25 mol% AlN by the reaction sintering in nitrogen gas at 1600–1800 °C, 20 MPa for 2 h[30]. Sintered $Al_2O_3$ with 1 mol% AlN

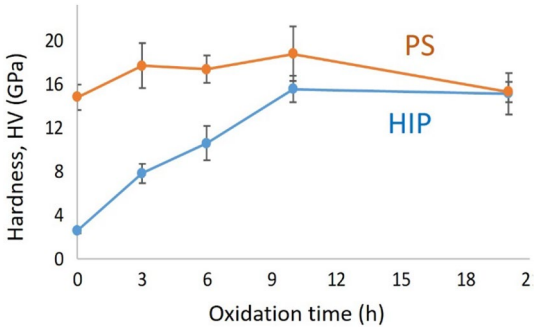


**Figure 10.** Hardness of HIP and PS sintered $Al_2O_3$ versus oxidation time of AlN base powder.

addition at 1750 °C resulted close to theoretical density of α-$Al_2O_3$ (3.98 g/cm3). They observed for the different compositions of AlN-$Al_2O_3$ that the sintered densities decreased with increasing AlN content[30].

Apparent density values of HIP and PS sintered $Al_2O_3$ are in agreement with results of group of Kim et al.[30]. The presence only the major α-$Al_2O_3$ predicted the higher densification during sintering process (independently on sintering type) (Fig. 9). AlN phase blocked the fully densification and caused the formation of the bigger grains, porosities and impurities in sintered ceramics (Figs. 4, 5, 6, 7, 8). The highest apparent density 3.39 g/$cm^3$ (85% relative density) has been observed in a case of sample oxidized for 10 h.

**Hardness of the sintered $Al_2O_3$.** The improvement of the mechanical properties of $Al_2O_3$ can be expected potential ceramics for novel engine or other applications. Hardness is one of the most important mechanical property.

Bocanegra-Bernal et al. obtained hardness of 20.5 ± 0.6 GPa presented a grain size of $Al_2O_3$ ~ 0.62 ± 0.04 μm at the lowest HIP temperature (1300 °C)[31]. Willmann reported the hardness values of 17–19 GPa for grain size of 4.5, 3.2, and 1.8 μm[32]. Xue et al. applied the hot pressing at various temperatures of 1800, 1850, and 1900 °C and produced the AlN-$Al_2O_3$ with hardness between 14 and 16 GPa[33].

Hardness values have been characterized as function of oxidation time (Fig. 10). The similar tendency of hardness behavior has been observed for both sintering techniques. The increasing of hardness has been influenced by increasing of oxidization time of base AlN powder, minimal presence of AlN and grain size of α-$Al_2O_3$. In addition, reduction of porosity resulted in closer packing, denser structure and improvement the hardness of sintered samples. The highest hardness values between 17 and 18 GPa have been observed for PS sintered α-$Al_2O_3$ oxidized between 3 and 10 h. These values are comparable with results of other research groups[31–33].

## Conclusions

Bulk sintered $Al_2O_3$ has been prepared by oxidization of AlN powder and combined sintering process, hot isostatic pressing (HIP) in $N_2$ and pressureless sintering (PS) in $H_2$ atmosphere. The HIP followed by PS post-sintering of oxidized AlN powder without sintering additives has been successfully developed for the first time. The micrometer sized AlN has been oxidized for 3, 6, 10 and 20 h in ambient atmosphere. The volume of $Al_2O_3$ increased with the increasing of oxidation time of AlN powder. Oxide layer caused porosities and the grains slightly growth. Above 10 h oxidation, "heat-treatment" metastable θ-$Al_2O_3$ phase has been observed. High temperature HIP sintering transformed θ-$Al_2O_3$ and only two major phases α-$Al_2O_3$ and minor AlN have been stabilized. PS post-sintering in 1800 °C for 10 h caused the phase transformation to α-$Al_2O_3$ which had effect on the apparent density and hardness of PS sintered ceramics. The highest apparent densities 3.11–3.39 g/$cm^3$ (78–85% relative densities) and highest hardness values (17–18 GPa) have been measured for PS sintered α-$Al_2O_3$ prepared from base powder oxidized between 3 and 10 h.

## Data availability

All data generated or analysed during this study are included in this published article.

Received: 14 February 2022; Accepted: 4 May 2022
Published online: 17 May 2022

## References

1. Kroke, E., Loeffler, L., Lange, F. F. & Riedel, R. Aluminum nitride prepared by nitridation of aluminum oxide precursors. *J. Am. Ceram. Soc.* **85**(12), 3117–3119. https://doi.org/10.1111/j.1151-2916.2002.tb00595.x (2002).
2. Baik, Y. & Drew, R. A. L. Aluminum nitride: Processing and applications. *Key Eng. Mater.* **124**(122–124), 553–570. https://doi.org/10.4028/www.scientific.net/kem.122-124.553 (1996).
3. Munro, R. G. Evaluated material properties for a sintered α-$Al_2O_3$. *J. Am. Ceram. Soc.* **28**(8), 1919–1928. https://doi.org/10.1111/j.1151-2916.1997.tb03074.x (1997).
4. Kresse, G. *et al.* Structure of the ultrathin aluminum oxide film on NiAl(110). *Science* **308**, 1440–1442. https://doi.org/10.1126/science.1107783 (2005).
5. Jeurgens, L. P. H., Sloof, W. G., Tichelaar, F. D. & Mittemeijer, E. J. Growth kinetics and mechanisms of aluminum-oxide films formed by thermal oxidation of aluminum. *J. Appl. Phys.* **92**(3), 1649–1656. https://doi.org/10.1063/1.1491591 (2002).

6. Jeurgens, L. P. H., Sloof, W. G., Tichelaar, F. D. & Mittemeijer, E. J. Structure and morphology of aluminium-oxide films formed by thermal oxidation of aluminium. *Thin Solid Films* **418**(2), 89–101. https://doi.org/10.1016/S0040-6090(02)00787-3 (2002).
7. Zheng, Y., Deng, Ch., Ding, J., Zhu, H. & Yu, Ch. Fabrication and microstructures characterization of AlN-$Al_2O_3$ porous ceramic by nitridation of $Al_4O_4C$. *Mater Charact.* **161**, 110159. https://doi.org/10.1016/j.matchar.2020.110159 (2020).
8. Osborne, E. W. & Norton, M. G. Oxidation of aluminum nitride. *J. Mater. Sci.* **33**, 3859–3865. https://doi.org/10.1023/A:1004667906474 (1999).
9. Yeh, C.-T. & Tuan, W.-H. Oxidation mechanism of aluminum nitride revisited. *J Adv. Ceram.* **6**(1), 27–32. https://doi.org/10.1007/s40145-016-0213-1 (2017).
10. Korbutowicz, R., Zakrzewski, A., Rac-Rumijowska, O., Stafiniak, O. & Vincze, A. Oxidation rates of aluminium nitride thin films: Effect of composition of the atmosphere. *J Mater Sci. Mater. Electron.* **28**(18), 13937–13949. https://doi.org/10.1007/s10854-017-7243-5 (2017).
11. Maghsoudipour, A., Moztarzadeh, F., Saremi, M. & Heinrich, J. G. Oxidation behavior of AlN–$Al_2O_3$ composites. *Ceram. Int.* **30**, 773–783. https://doi.org/10.1016/j.ceramint.2003.10.004 (2004).
12. Cao, Y. *et al.* Microstructure, growth kinetics and formation mechanism of oxide layers on AlN ceramic substrates. *J. Ceram. Sci. Technol.* **9**(3), 263–270. https://doi.org/10.4416/JCST2018-00011 (2018).
13. Min, J.-H., Lee, J. & Yoon, D.-H. Fabrication of transparent γ-AlON by direct 2-step pressureless sintering of $Al_2O_3$ and AlN using an AlN-deficient composition. *J Eur. Ceram. Soc.* **39**, 4673–4679. https://doi.org/10.1016/j.jeurceramsoc.2019.07.030 (2019).
14. Manabe, Y., Fujikawa, T., Ueda, M. & Inoue, Y.: Effect of $O_2$-HIP for oxide ceramics. In: First European ceramic society conference held at Maastricht, Netherlands, 18–23 June 1989.
15. Prosvirnin, D. V., Kolmakov, A. G., Larionov, M. D., Prutskov, D. E. & Levina, A. V. Methods and techniques for producing ceramics from aluminum oxynitride. *IOP Conf. Ser. Mater. Sci. Eng.* **525**, 012. https://doi.org/10.1088/1757-899X/525/1/012067 (2019).
16. Varanasi, D., Furkó, M., Balázsi, K. & Balázsi, C. Processing of $Al_2O_3$-AlN ceramics and their structural, mechanical, and tribological characterization. *Materials* **14**(20), 6055. https://doi.org/10.3390/ma14206055 (2021).
17. Li, M. *et al.* Effect of hydrogen on the integrity of aluminium–oxide interface at elevated temperatures. *Nat. Commun.* **8**(2017), 14564. https://doi.org/10.1038/ncomms14564 (2017).
18. Anya, C. C. & Roberts, S. G. Pressureless sintering and elastic constants of A10-SIC nanocomposites. *J. Eur. Ceram. Soc.* **17**, 565–573. https://doi.org/10.1016/S0955-2219(96)00092-1 (1997).
19. Tuan, W. H., Lin, M. C. & Wu, H. H. Preparation of $Al_2O_3$Ni composites by pressureless sintering in $H_2$. *Ceram. Int.* **21**(4), 221–225. https://doi.org/10.1016/0272-8842(95)99785-A (1995).
20. Tabary, P., Servant, C. & Alary, J. A. Microstructure and phase transformations in the AlN-$Al_2O_3$ pseudo-binary system. *J. Eur. Ceram. Soc.* **20**, 913–926. https://doi.org/10.1016/S0955-2219(99)00238-1 (2000).
21. Katnani, A. D. & Papathomas, K. I. Kinetics and initial stages of oxidation of aluminum nitride: Thermogravimetric analysis and X-ray photoelectron spectroscopy study. *J. Vac. Sci. Technol. A* **5**, 1335–1340. https://doi.org/10.1116/1.574765 (1987).
22. Suryanarayana, D. Oxidation kinetics of aluminum nitride. *J. Am. Ceram. Soc.* **73**, 1108–1110. https://doi.org/10.1111/j.1151-2916.1990.tb05167.x (1990).
23. Brown, A. L. & Norton, M. G. Oxidation kinetics of AlN powder. *J Mater. Sci. Lett.* **17**, 1519–1522. https://doi.org/10.1023/A:1006512904173 (1998).
24. Zhou, H., Qiao, L. & Fu, R. Effect of the fluoride additives on the oxidation of AlN. *Mater. Res. Bull.* **37**, 2427–2435. https://doi.org/10.1016/S0025-5408(02)00942-X (2002).
25. Uematsu, K. *et al.* Hot isostatic pressing of alumina and examination of the hot isostatic pressing map. *J. Am. Ceram. Soc.* **73**(1), 74–78. https://doi.org/10.1111/j.1151-2916.1990.tb05093.x (1990).
26. Manabe, Y., Fujikawa, T. & Narukawa, Y.: Effect of $O_2$-HIP for oxide ceramics. In: Second international conference on hot isostatic pressing—theory and applications, National Institute of Standards and Technology, Gaithersburg, Maryland, USA, 7–9 June 1989.
27. Xu, X. R., Yan, W. L., Zhuang, H. R., Li, W. L. & Xu, S. Y. Oxidation behavior of aluminum nitride. *Wuji Cailiao Xuebao/J. Inorg. Mater.* **18**(2), 337–342 (2003).
28. Besson, J. & Abouaf, M. Grain growth enhancement in alumina during hot isostatic pressing. *Acta Metall.* **39**, 2225–2234. https://doi.org/10.1016/0956-7151(91)90004-K (1991).
29. MacKenzie, K. J. D., Temuujin, J., Smith, M. E., Angerer, P. & Kameshima, Y. Effect of mechanochemical activation on the thermal reactions of boehmite (γ-AlOOH) and γ-$Al_2O_3$. *Thermochim. Acta* **359**(1), 87–94. https://doi.org/10.1016/S0040-6031(00)00513-X (2000).
30. Y.W. Kim, H.C. Park, Y.B. Lee, K.D. Oh, Stevens, R. Reaction sintering and microstructural development in the system $Al_2O_3$–AlN, *J. Eur. Ceram. Soc.* 21(2001) 2383–2391. https://doi.org/10.1016/S0955-2219(01)00200-X
31. Bocanegra-Bernal, M. H. *et al.* Hot isostatic pressing (HIP) of a-$Al_2O_3$ submicron ceramics pressureless sintered at different temperatures: Improvement in mechanical properties for use in total hip arthroplasty (THA). *Int. J Refract. Met. Hard Mater.* **27**, 900–906. https://doi.org/10.1016/j.ijrmhm.2009.05.004 (2009).
32. Willmann, G. Ceramic femoral head retrieval data. *Clin. Orthop. Relat. Res.* **379**, 22–28 (2000).
33. Xue, J. M. *et al.* Hot-pressed translucent aluminum oxynitride (AlON) ceramics. *Key Eng. Mater.* **368–372**, 450–452. https://doi.org/10.4028/www.scientific.net/KEM.368-372.450 (2008).


## Acknowledgements

The authors sincerely thank to colleagues from Centre for Energy Research, namely Viktor Varga for helping us in carrying out the sample preparation, Noémi Szász and Levente Illés for helping us in the SEM analysis of the samples, András Hiripi (Tungsram Operations Ltd.) for pressureless sintering of samples. This research was funded by the Hungarian National Research Development and Innovation Office (project NKFIH-NNE 129976).

## Author contributions

Conceptualization, design of experiments C.B. and K.B.; methodology, D.V. and F.C.S; investigation, interpretation of data for the work, validation D.V., Zs.E.H, and M.F.

## Funding

Open access funding provided by Centre for Energy Research.

## Competing interests

The authors declare no competing interests.

## Additional information

**Correspondence** and requests for materials should be addressed to K.B.